

# HGHG AND EEHG MICROBUNCHES WITH CSR AND LSC\*

Kirsten Hacker, TU Dortmund, Germany

## Abstract

Longitudinal space charge (LSC) forces in a drift and coherent synchrotron radiation (CSR) in a chicane are relevant for high gain harmonic generation (HGHG) and echo enabled harmonic generation (EEHG) seeding designs. These factors determine whether or not the modulator can be located significantly upstream of the radiator. The benefits and dangers of having a drift in between the radiator and the modulator are investigated and a measurement of the LSC enabled reduction of the energy spread of a seeded beam is presented.

## INTRODUCTION

The length of a seeded microbunch determines the harmonic content and the harmonic content together with the energy spread determines the shortest wavelength which the system can seed [1-3]. For a given initial uncorrelated energy spread, the length of a microbunch can be reduced by increasing the modulation amplitude, but when the modulation amplitude becomes too great, the energy spread of the microbunches will be too large to lase in the radiator [4]. In addition, microbunches with high peak currents will be subject to significant coherent synchrotron radiation (CSR) in the chicane and longitudinal space charge (LSC) forces in the drift [5,6]. For FLASH2 seeding, a decision about where an HGHG modulator should be placed is determined by how these factors influence the behavior of an HGHG microbunch in a drift. This material was first presented in [7,8]. It represents an initial investigation into this design issue for FLASH2. The full-bunch simulation methods from [9] would be used in a final design study.

Two possible configurations of a FLASH2 seeding installation are drawn in Fig. 1. Option (a.) has the HGHG modulator in the middle of the radiator, minimizing the drift of the microbunched electrons and option (b.) has the modulator at the beginning of the radiator, necessitating a 20 meter drift of an energy modulated electron bunch prior to beginning the radiation process. This drift is required due to the short length of undulator required to achieve saturation in a seeded FEL and due to the necessity of keeping the saturation point at a fixed point in the radiator for longer wavelengths. If the beam saturates too early in the radiator, then the 20-30 nm FEL light cannot be transported to the users.

In order to determine which option is superior, longitudinal dispersion, longitudinal-transverse coupling, coherent synchrotron radiation (CSR), and longitudinal space charge (LSC) all need to be addressed. The conclusion from a study of these issues is that option (a.), with the modulator in the middle of the radiator, suffers

\* work supported by BMBF grant 05K10PE1 and DESY

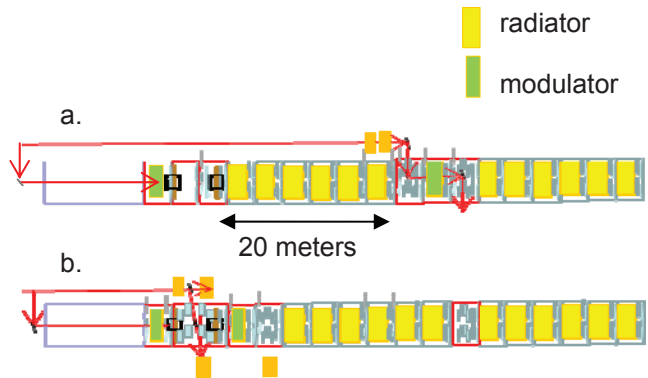


Figure 1: Two possible locations for an HGHG modulator in a FLASH2 seeding installation. Option (a.) shows it in the middle of the radiator in a design which is only suitable for HGHG and option (b.) shows it prior to the radiator in a design which is suitable for a wider range of seeding schemes. The additional, upstream modulator is envisioned for EEHG.

most from CSR, while option (b.), given more ample seed laser intensity, can exploit LSC forces in a beneficial manner, using them to reduce the net energy spread of the microbunches. Measurements and simulations of this LSC enabled increase of the microbunch energy spread concept are presented. Conversely, measurements of the LSC enabled enhancement of a microbunch energy spread are presented in [10] with a different application. Whether or not the LSC force enhances or reduces the microbunch energy spread depends on whether the microbunch is undercompressed or overcompressed at the entrance of a drift.

## DISPERSION

The energy modulated beam is affected by dispersion from the chicanes, from the modulator, from mis-aligned magnets or beam trajectories, and from the velocity bunching in the drift itself. Higher order dispersion becomes relevant for large energy modulations in terms of its effect on coupling between longitudinal and horizontal dispersion for non-closed orbit bumps. It will be discussed in the section on 3-D effects. A table summarizing the first-order dispersion ( $R_{56} = 2\Delta s$ ) contributions for a 20 meter drift is given below (Table 1).

Table 1: A summary of the contributions to the dispersion over a 20 meter drift for a beam energy of 700 MeV and a trajectory mis-alignment of 100  $\mu\text{m}$  and modulator with 30 periods.

velocity	$L_{drift} / \gamma^2$	15 $\mu\text{m}$
mis-alignment	$L_{drift} \theta^2$	5 nm
modulator	$2N_{periods} \lambda_{seed}$	16 $\mu\text{m}$
chicane	$(L_{chicane} - 3L_{bend}) \theta^2$	0-200 $\mu\text{m}$

For an overly large, 4 MeV energy modulation, the dispersion required to fully bunch the beam is about 20  $\mu\text{m}$ , while for a more reasonable, 2 MeV energy modulation, the dispersion required for full compression is 50  $\mu\text{m}$ . Since the dispersion in the drift is sufficient to compress a beam with a larger energy modulation, for option (a.), the CSR of the chicane will be dominant, while for option (b.), the LSC of the drift dominates.

### CSR AND LSC

Analytic equations [5,6] for CSR and LSC forces can be added to a quick 1-D tracking code by applying the forces to a few microbunches and tracking the particle motion over a drift. The CSR wakes are calculated for the last dipole in the chicane prior to the radiator and the LSC forces are calculated for a given distance, using an interval of 1 meter per re-calculation.

To determine the fraction of the last dipole which is relevant for the CSR calculation, the point at which transverse smearing becomes small must be identified. The metric is that when the longitudinal-transverse smearing ( $\sigma_{x,y}$ ) times  $R_{53}$  is larger than the length of the microbunch, then the peak current of the microbunch is low and the CSR can be ignored. Plotting the smearing and the  $R_{53}$  along the chicane shows that for  $\beta=20$  m,  $\varepsilon=1.5$ , and a 100  $\mu\text{m}$  (rms) beam radius,  $\sigma_{x,y} \cdot R_{53} = 6$  nm at the dipole entrance, implying that the entire length of the last dipole is relevant for a 10 nm long HGHG microbunch. Only the last half would be relevant for a shorter, EEHG microbunch (Fig. 2).

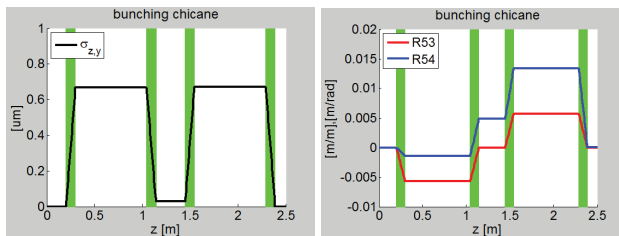


Figure 2: Longitudinal-transverse smearing ( $\sigma_{x,y}$ ) and  $R_{53}$  along the chicane. This shows that for a 10 nm microbunch, only the last half of the last dipole is relevant for a CSR calculation.

In option (a.), the bunching is accomplished primarily through the chicane directly after the modulator, making CSR the primary concern whereas, in option (b.), the compression is done mostly through dispersion in the drift making LSC a larger concern. For option (a.), CSR from an electron bunch with an energy modulation of 2 MeV in the last dipole of a 45  $\mu\text{m}$  chicane is studied after a drift of 4 meters with an average beam radius of 100  $\mu\text{m}$  (rms). This gives a picture of the microbunch after the exit of the first radiator segment. For option (b.), the impact of LSC is studied over a drift of 20 meters with an average beam radii of 100  $\mu\text{m}$  (rms) and 200  $\mu\text{m}$  (rms). 2 MeV and 4 MeV energy modulations are compared for a beam energy of 600 MeV and 1 kA initial peak current.

In Fig. 3, the longitudinal phase space of the electrons in a microbunch for option (a.) is plotted along with the projection onto the longitudinal axis. The 2 sigma energy spread limits of the radiator are depicted by dashed lines. The background particles in blue show the conditions prior to the application of CSR and LSC. The foreground, red particles show the bunch after CSR and LSC and 4 meters of drift. The green line shows the LSC force per meter.

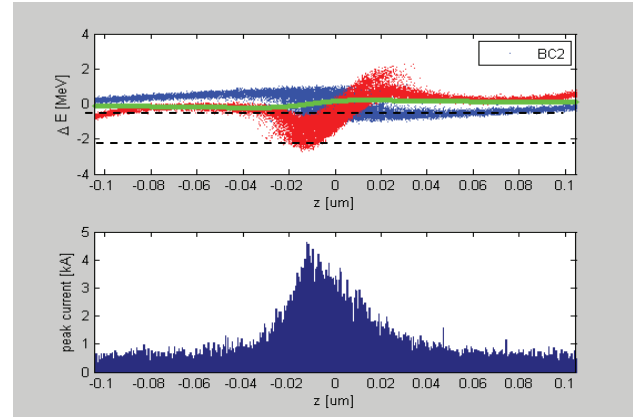


Figure 3: LSC and CSR on a microbunch after 4 meters of drift and an  $R_{56}$  of 45  $\mu\text{m}$ . Dashed lines represent the bandwidth of the radiator. The background particles in blue show the conditions prior to the application of CSR or LSC. The foreground, red particles show the bunch after CSR and LSC and 4 meters of drift. The green line gives the LSC potential per meter. This is done for a 700 MeV beam energy, 1 kA initial peak current, 2 MeV (pp) energy modulation and a chicane  $R_{56}$  of 45  $\mu\text{m}$ . The harmonic content of the microbunch was unaffected, but the energy spread was increased.

In contrast to the case of option (a.) plotted above in Fig. 3, option (b.) would send the energy modulated beam through a drift of 20 meters prior to the bunching chicane. If the beam radius is 100  $\mu\text{m}$  in the drift, then the LSC wake will completely erase, or even reverse a 2 MeV initial energy modulation (Fig. 4) making seeding impossible with this amount of energy modulation and LSC potential.

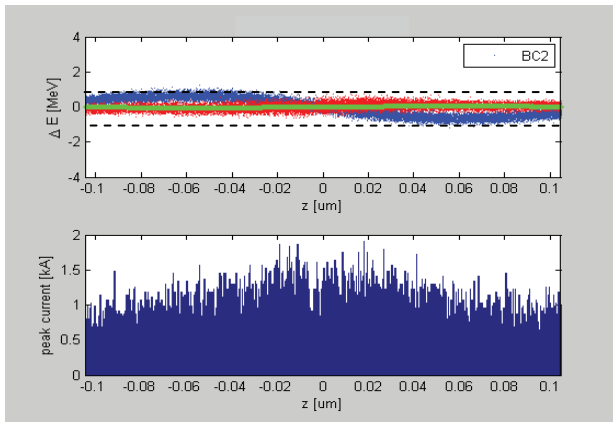


Figure 4: For a 100 μm (rms) radius, 1 kA electron bunch with a beam energy of 700 MeV and an initial energy modulation of 2 MeV (pp), the LSC potential completely removes the initial energy modulation after 20 meters of drift (blue ->red). LSC potential per meter is green.

If, however, the initial energy modulation is increased to 4 MeV, then one observes an LSC plasma oscillation which bunches the beam in the drift alone (Fig. 5).

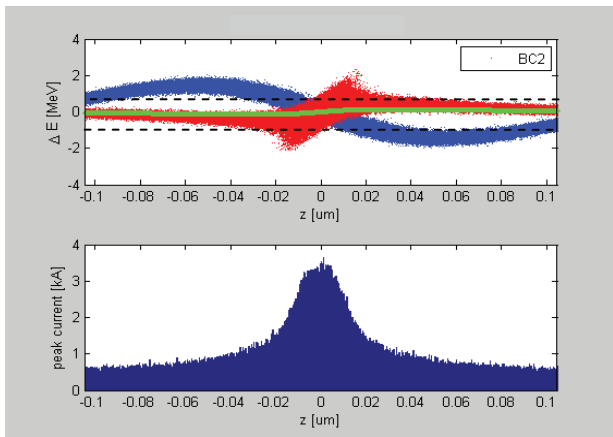


Figure 5: Instead of compression through a chicane, the energy modulated beam develops microbunches as a result of the LSC potential along the drift. The average rms beam radius in the 20 meter drift was 100 μm for a 1 kA initial peak current.

Such an LSC compressed microbunch would have a high enough peak current to radiate in an FEL were it not for the fact that the chirp is positive instead of negative, meaning that any amount of dispersion will blow the microbunch apart. This is not a workable scheme.

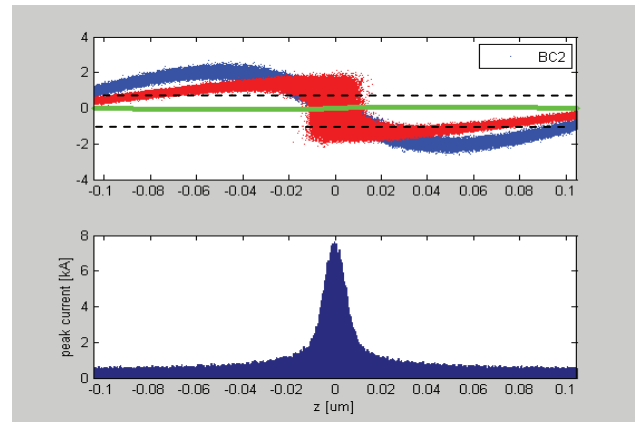


Figure 6: By increasing the beam radius in the 20 meter drift to 200 μm (rms) so that the time-of-flight compression dominates over the LSC force, a microbunch with a reduced peak-to-peak energy modulation is produced.

If the average beam radius in the drift is increased to 200 μm from 100 μm, so that the compression through the time-of-flight in the drift dominates over the effect of the LSC force, then an ideal condition appears to be realized. The beam is compressed without CSR and with an LSC enabled reduction of the peak-to-peak energy modulation (Fig. 6). This reduction of the seeded beam’s energy spread improves the performance in FEL radiator, reducing the gain length and increasing the maximum power radiated.

An important tolerance for microbunch compression in a drift is the dispersion leakage in the drift. If the  $R_{53}$  and  $R_{54}$  are non-zero in the drift, as in a closed orbit bump, then the microbunches will be transversely smeared out in the drift and the effect of the LSC force will be dramatically attenuated. With this in mind, the strength of the LSC wake might be fine-tuned through closed orbit bumps instead of by tuning the beam size in the drift.

### 3-D SIMULATIONS

All of the previous results are merely 1-D simulations with an LSC force which is calculated from the longitudinal charge density. Simulations that calculate the forces between particles with a Green’s function algorithm in 3-D [11] show some additional smearing effects which are not present in the 1-D simulations from Figs. 5 and 6. The effects shown in Fig. 5 and 6 are reproduced in 3-D but with a reduction in the peak current of the microbunch compared to the 1-D results (Fig. 7).

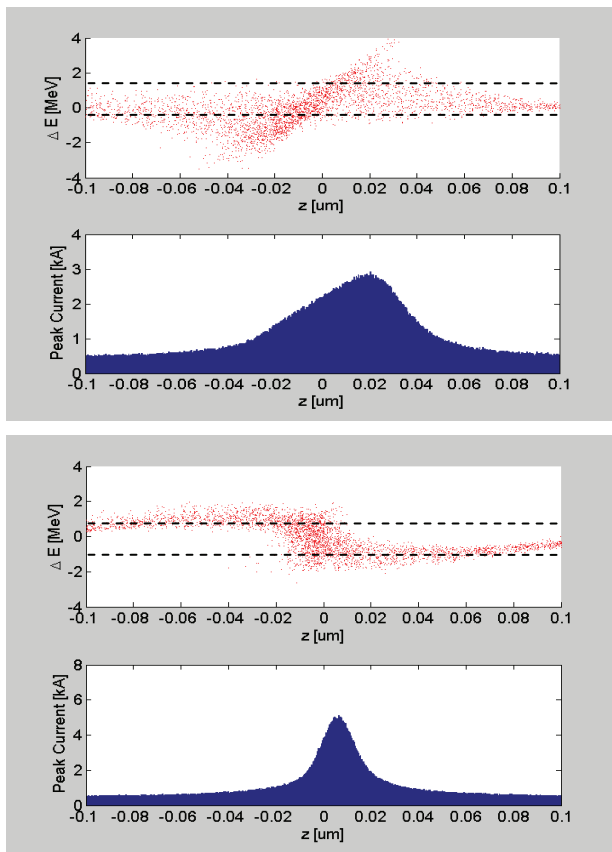


Figure 7: 3-D simulation of conditions from Figs. 5 and 6. The same mechanism is observed, but, due to 3-D smearing effects in the simulation, less impressive peak current is seen. (a.) has a beam radius of  $100\ \mu\text{m}$  in the drift and (b.) has a beam radius of  $200\ \mu\text{m}$  in the drift

The harmonic content of the microbunch in Fig. 7, representative of option (b.) is sufficient for seeding up to the 12<sup>th</sup> harmonic of 266 nm, while the harmonic content of the microbunch from Fig. 3, representative of option (a.) has comparable harmonic content. Each result is consistent with the observation of seeding up to the 12<sup>th</sup> harmonic of 266 nm at ELETTRA with an initial slice energy spread of 150 keV [12]. This allows us to draw a conclusion for HGHG that given ample seed intensity, option (a.) is inferior to option (b.) since the energy spread of the microbunches is larger. However, given limited seed intensity, option (a.) is superior for HGHG. EEHG requires different considerations.

### EEHG

A comparison of option (a.) and option (b.) should also be done with respect to their compatibility with EEHG. Based on Fig. 8, an EEHG folded and energy modulated beam with 1 kA of initial peak current and a  $100\ \mu\text{m}$  average radius cannot tolerate the 20 meters of drift required by option (b.). Blue represents a slice of the seeded electron beam prior to the drift and red is after the drift.

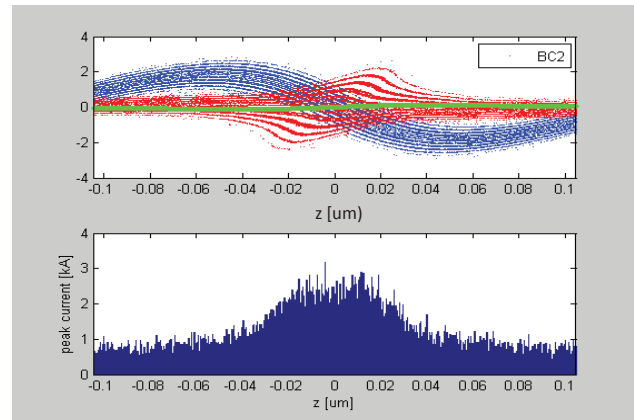


Figure 8: An EEHG folded and energy modulated 1 kA beam cannot be transported over 20 meters of drift in option (b.). The average transverse beam radius for this simulation was  $100\ \mu\text{m}$ . Blue represents a slice of the seeded electron beam prior to the drift and red is after the drift.

To avoid the problem with option (b.) shown in Fig. 8, the EEHG microbunches could be compressed directly after modulation, keeping the distance between the chicane exit and the radiator entrance as small as possible. Then, a split radiator scheme would be used in order to transport the FEL radiation to the users. Alternatively, the microbunches might be transported in a closed orbit bump which uses the  $R_{53}$  and  $R_{54}$  to keep the charge density transversely smeared out so that the LSC wake cannot have the effect shown in Fig. 8.

In option (a.), the folded beam would be transported over the 20 meter drift without the second stage energy modulation shown in blue in Fig. 8. In this case, due to inhomogeneities in the longitudinal charge density which are present after the initial EEHG folding (Fig. 9), effects akin to the LSC-EEHG described in [13] could occur and ruin the effectiveness of the EEHG seeding process.

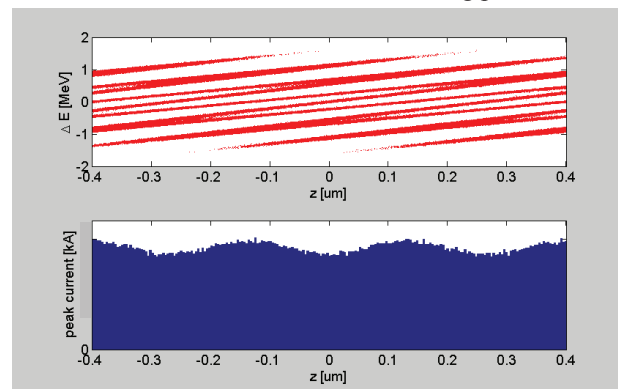


Figure 9: Folded beam distribution in longitudinal phase space. For option (a.), the small variations in the peak current after the first EEHG modulation and folding would introduce distortions due to the LSC force in a long drift.

For option (a.) or (b.), the average beam radius,  $R_{53}$  and  $R_{54}$  in the drift could be increased to avoid the damaging LSC effects for EEHG. However, only option (b.) offers

the possibility to avoid the LSC problem through a split radiator concept. Only option (b.) is consistent with a fresh-bunch cascade technique.

## MEASUREMENT

Measurements of the LSC enabled reduction of the energy spread of a microbunched portion of the beam were performed at FLASH during shifts for a study of SASE lasing suppression [10,14]. The shift conditions used 300 A instead of the 1 kA from simulations shown above and simulations and measurements of longitudinal phase space of the un-bunched, under-bunched, and bunched conditions of the seeded beam are shown in Fig. 10.

The longitudinal phase space measurement was conducted with an RF deflecting structure which streaks out the longitudinal structure of the electron bunch in the vertical direction. A dipole magnet streaks out the energy of the bunch in the horizontal direction. The data analysis tool prepared by [15] was used to interpret the images.

The  $R_{56}$  of the chicane directly after the modulator was scanned from zero up to 100  $\mu\text{m}$ . For  $R_{56}$ s below 50  $\mu\text{m}$ , the energy modulation was a constant 2 MeV (pp) (Fig. 10a), but at 50  $\mu\text{m}$  a transition occurred. The energy modulation disappeared at  $R_{56}=50 \mu\text{m}$  (Fig. 10b). This is due to the LSC potential acting to reduce the energy spread of the microbunches as described in the simulation shown in Fig. 4. As the  $R_{56}$  was increased above 50  $\mu\text{m}$ , the energy modulation returned, but in a new form (Fig. 10c). Three regions of streaked charge are observed, while in Fig. 10a, only one region is present. This is due to the fact that the peak current of the microbunches varies more along the seeded portion of 10c, leading to different amounts of LSC potential and modification of the microbunch energy spread along the drift.

## CONCLUSION

The issues of LSC in a drift and CSR in a chicane are relevant for HGHG and EEHG seeding designs. Based on a comparison of two designs: one with the HGHG modulator in the middle of the radiator and one with it prior to the radiator, the favored design puts the modulator prior to the radiator due to increased flexibility in operation techniques including a split radiator concept, a fresh bunch cascade concept. The primary benefit may be the possibility of an LSC assisted energy spread reduction concept for HGHG.

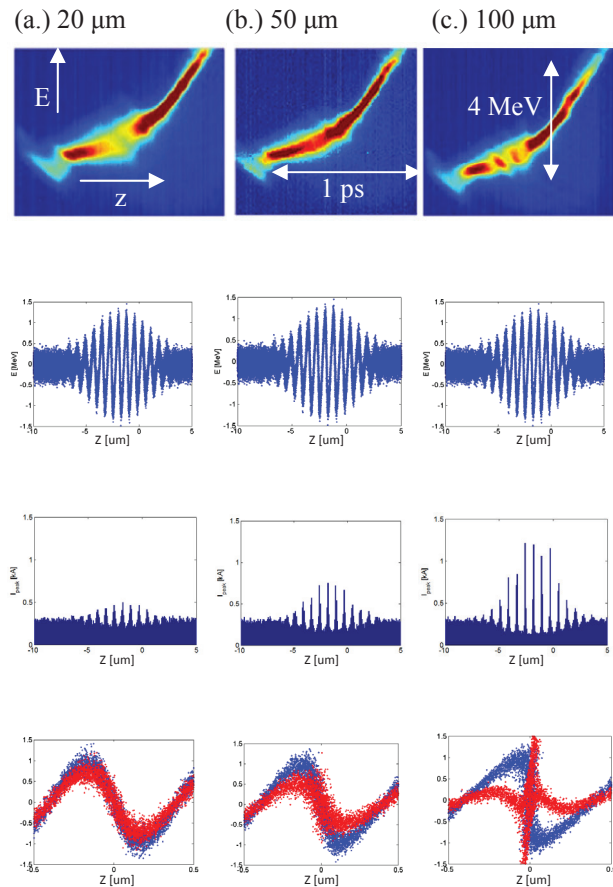


Figure 10: The longitudinal phase space for 3 different chicane  $R_{56}$ s measured with RF deflecting structure. The beam energy was 700 MeV and the peak current was 300 A. In (a), the microbunch is only slightly compressed, in (b), the microbunch is almost fully compressed, and in (c), the microbunch is over-compressed in the center of the seed. Simulations of the seeded microbunches are shown below. The seed pulse length has been shortened by a factor of 6 in the simulation, so that the individual bunches are visible. Red dots are after the drift, blue dots are before the drift.

## ACKNOWLEDGEMENTS

The author would like to thank Bart Faatz for information about the FLASH2 layout, Velizar Miltchev for his perspective on FLASH2 design, Martin Dohlus for his 3-D LSC code, Holger Schlarb for initial education on several topics, and the operations team [9] for allowing the measurement during beam time allocated for another purpose.

## REFERENCES

- [1] L.H. Yu, Phys.Rev. A 44,5178 (1991).
- [2] V.V. Goloviznin and P.W. van Amersfoort, Phys.Rev.E 55, 6002 (1997).
- [3] H.X. Deng and Z.M. Dai, Chinese Phys. C 34, 1140 (2010).
- [4] P. Schmueser, et al., Springer (2008).

- [5] E.L. Saldin, E.A. Schneidmiller, and M.V. Yurkov, DESY Reports, TESLA-FEL 1996-14
- [6] Z. Huang, et al., Phys. Rev. STAB 7, 074401 (2004).
- [7] K. Hacker, “Seeding FLASH between 4 and 40 nm”, FLASH seminar 2013 (Nov, 12 2013).
- [8] K. Hacker, DESY Reports, TESLA-FEL 2013-01.
- [9] G. Feng, et al., These Proceedings: Proc. 36th Int. Free-Electron Laser Conf., Basel, 2014, MOP083.
- [10] C. Lechner et al., These Proceedings: Proc. 36th Int. Free-Electron Laser Conf., Basel, 2014, MOP060.
- [11] M. Dohlus, “Q-solver”, DESY FEL beam dynamics group webpage, <http://www.desy.de/fel-beam/>.
- [12] E. Allaria et al., Nat. Photon. 7, 913 (2013).
- [13] K. Hacker, to-be-published, PRST-AB Sept. 2014.
- [14] Operators for Measurements: S. Ackermann, J. Boedewadt, N. Ekanayake, K. Hacker, C. Lechner, T. Maltezopelous.
- [15] Christopher Behrens, Dissertation, Fachbereich Physik der Universität Hamburg, 2012.